ISAR IMAGES GENERATION VIA GENERATIVE ADVERSARIAL NETWORKS

*Ruo-Yi Zhou, Zhi-Long Yang and Feng Wang**

Key laboratory for Information Science of Electromagnetic Waves (MoE),
School of Information Science and Technology, Fudan University, Shanghai 200433, China.
ryzhou19@fudan.edu.cn, zlyang18@fudan.edu.cn
**Corresponding author*: fengwang@fudan.edu.cn

IGARSS 2021 - 2021 IEEE International Geoscience and Remote Sensing Symposium | 978-1-6654-0369-6/21/$31.00 ©2021 IEEE | DOI: 10.1109/IGARSS47720.2021.9553814

ABSTRACT

One of the challenges faced by current intelligent target recognition tasks is the lack of samples, especially in the Inverse Synthetic Aperture Radar (ISAR) images understanding. In this paper, we proposed an ISAR objects generative network to generate multi-aspect ISAR images. A simulated ISAR dataset of six types of aircrafts is produced via, using bidirectional analytic ray tracing (BART) method. Then, the proposed generative network is trained with the simulated ISAR dataset. We evaluated the performance of the proposed network using structural similarity (SSIM). The experimental results show that the generated targets are very close to the real ISAR samples, and the SSIM between generated and real ISAR images of aircrafts is larger than 0.7.

Index Terms— Inverse Synthetic Aperture Radar (ISAR), Automatic Target Recognition (ATR), Generative Adversarial Nets (GANs)

1. INTRODUCTION

High-resolution Inverse Synthetic Aperture Radar (ISAR) imaging, which can work under all-day and all-weather conditions, has been proved as a useful technology to monitor the moving aerial targets[1]. Recently, deep-learning methods such as Convolutional Neural Networks (CNN), faster RCNN (Regions with CNN feature), has been extensively applied in the remote sensing imagery interpretation [2]. Usually, intelligent classification of remote sensing imagery with deep learning methods need adequate training samples that cover full-aspect orientation angles. In practical use, it is difficult to obtain enough training samples.

Generative Adversarial Nets (GANs) [3] has also been introduced to SAR images generation tasks for its high fidelity images generation ability [4]. GANs can expand the number of ISAR imaging results in the azimuth dimension, and shows great potential in addressing the shortage of ISAR imagery dataset. Furthermore, augmented ISAR data can improve the recognition and classification accuracy. GANs has been extensively applied in remote sensing target generation. For example, Conditional Generative Adversarial Nets (CGANs) [5] is used to generate SAR images from optical ones [6]. And experiments have been carried out with the MSTAR (Moving and Stationary Target Acquisition and Recognition) [4] [7].

In this paper, an ISAR simulation imagery dataset is constructed using the bidirectional analytic ray tracing (BART) electromagnetic scattering calculation tool [8]. By BP (Back-Projection) imaging algorithm, 2160 ISAR images crops of moving aerial targets have been derived from the raw simulation data. Besides, an ISAR image generation network is adopted to interpolate the images along orientation dimension, so that the number of training samples is greatly increased. The generative network is trained on dataset with few ISAR images, but be able to generate massive ISAR images of aerial targets with other orientations. The test set in ISAR simulation dataset is furtherly used to evaluate the generation performance of the generative network.

The paper is organized as follows. Section 2 describes the generative network used to augment the ISAR image dataset. Section 3 introduces the simulation of ISAR imaging. In section 4, the experimental results are demonstrated. And we give the conclusions in section 5.

2. ISAR IMAGE GENERATIVE NETWORK

In this section, GAN [9] [10] is adopted to interpolate the ISAR images along the orientation dimension, as inspired by recently developed SAR image generative network [4].

GANs simultaneously train two subnetworks: a generative network *G* which captures the data distribution; a discriminative network *D*, which estimates the probability that the input image comes from the original data. The training procedure for *G* is to maximize the mistake probability of *D*. Then we train *D* to maximize the probability that the category and angle of the images generated from G is correct. And the loss function of GAN is defined as,

$$\mathcal{L}_{GAN} = \min_{G}\max_{D} \mathbb{E}_{X}[D(X)] - \mathbb{E}_{z\sim p(data)}\left[D\left(G\left(z, v, c; \theta_g\right)\right)\right] \quad (1)$$

where z is the input vector that sampled from a Gaussian distribution, $D(x)$ is the probability that x comes from the real data, and $G\left(z, v, c; \theta_g\right)$ representing a mapping to data space where *G* is a differentiable function represented by a

neural network with parameter θ_g.

After adding the orientation angle and label to the inputs of the generator (shown in Fig. 1), the overall architecture of the network is illustrated in Fig. 2. The network contains two main structures, which is similar to basic GANs, i.e. generator and discriminator. The difference is, two additional inputs of angle vector $v = [\cos\phi, \sin\phi]^T$, and one-hot label vector c in the generator are used to specify the angle and categories of the generated ISAR imagery.

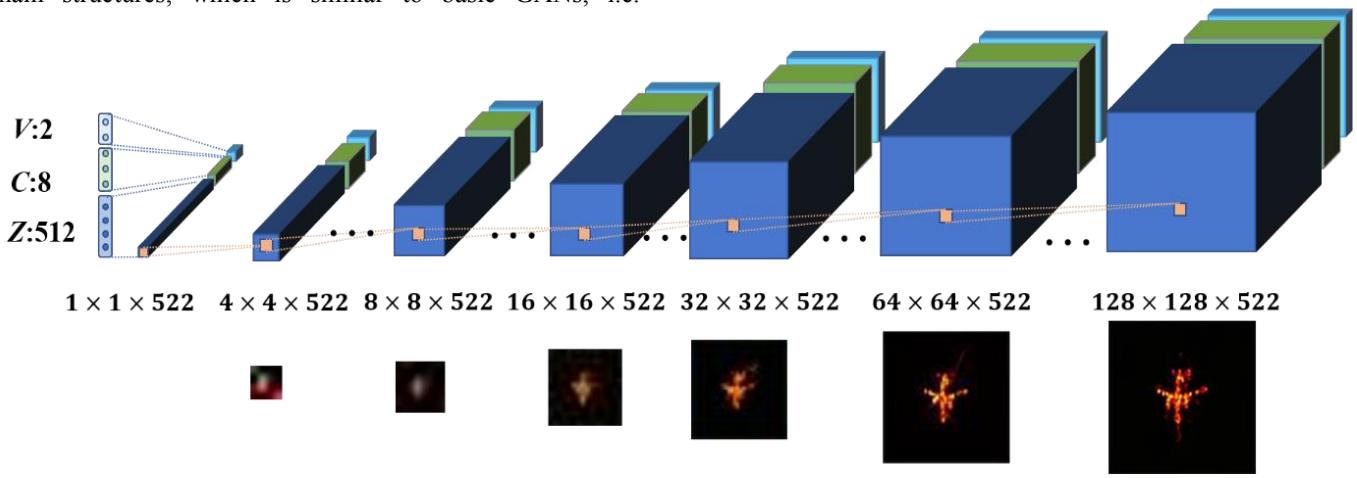

Fig. 1. Progressive growing form of GANs' generator with limited input vectors *v* and *c*.

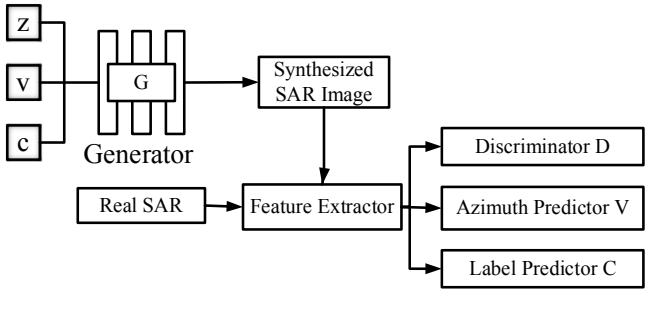

Fig. 2. The architecture of adopted GANs.

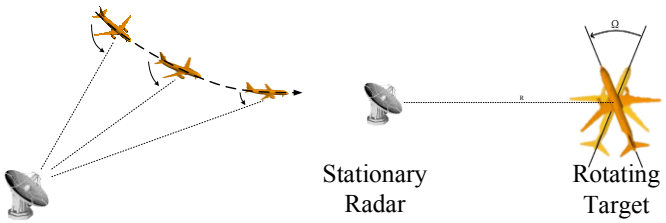

Fig. 3. Geometry of ISAR imaging.

3. SIMULATION OF ISAR IMAGING

As shown in Fig. 3, different from SAR system, radar in ISAR keeps stationary, and is used to detect the moving target. ISAR has the ability to discriminate different targets, which makes it of great use in space target recognition [1]. The range and azimuth resolution of 2-D ISAR image depends on the bandwidth, wavelength etc.,

$$\delta_r = c/2B, \qquad \delta_a = c/(2f_c\Omega) \tag{2}$$

where c is the speed of light; B and f_c are the bandwidth and the center frequency of electromagnetic wave respectively; Ω is the angular bandwidth. Fig. 4 compares the simulated (first and third rows) and the optical (second and last row) images of eight categories of aircrafts, in the simulated ones, the radar is diagonally bellowing the plane.

Table I Parameters of the ISAR imaging.

Parameter	Quantity
f_c(Center of frequency)	9.65 GHz
B(Bandwidth)	300 M
Number of frequencies	241
Resolution in range direction	0.5 m
Angular width	1.78°
Number of azimuth angles	241
Resolution in azimuth direction	0.5 m
Elevation angle	45°

Fig. 4. Simulated ISAR images and corresponding optical images of eight types of aircraft.

The recent developed recognition algorithms, especially those based on deep learning methods, depend greatly on the available training data [2]. However, to our knowledge, there is still no open-sourced practical ISAR datasets which can cover full-aspect angles. An ISAR image set of six aircrafts (i.e. Airbus-220, Airbus-320, Boeing-737, Boeing-747, Boeing-777, Boeing-787) that covers all aspect orientation (0~360°) is conducted in this paper. The dataset is then used to boost the ISAR target recognition algorithm. BART method [8] is adopted to compute the scattering from aircraft targets. The simulation parameters are listed in Table I.

Due to the coherent imaging mechanism of ISAR, the images of same targets under different orientation vary a lot. Fig. 5 shows the examples of simulated full-aspect ISAR images of small and large aircrafts separately with spatial resolution of 0.5 m.

4. RESULTS AND ANALYSIS

In this section, the simulated ISAR images in section 3 are used to validate the generative network in section 2. The radar is diagonally below the plane. The elevation angle is 45°. The ISAR images are split into training and test sets in terms of the orientation angles. The training data are firstly picked out so that the orientation interval between any two samples of the same target is larger than 12°. The other part data is used as test set. The training data are then used to train the proposed generative network.

We compare the simulated ISAR images in training set (Fig. 6a) with the corresponding generated ISAR images (Fig. 6b). Results show that the generated ISAR images are consistent with the simulated ones. The trained generative network can be used to interpolate between any two adjacent images in the orientation dimension. In Fig. 7, we compare the real ISAR images (top row) from test set with interpolated ones (bottom row), which are generated by the generator. Images in the left and right columns are from training data. Comparison shows that the proposed generative network can be well used in generating high resolution ISAR images in missing angles, which remain similar to the real ones.

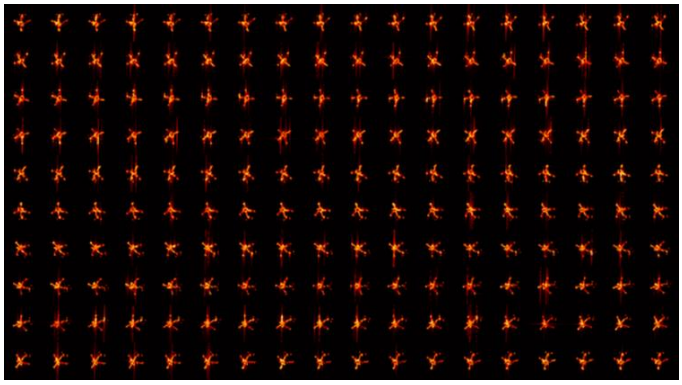

Fig. 5. Full-aspect simulated ISAR images of Boeing-737.

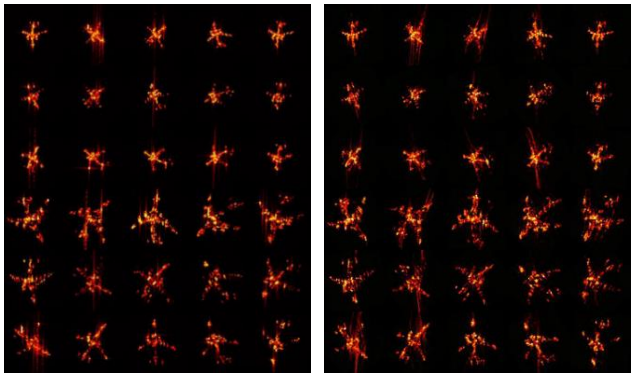

(a) (b)

Fig. 6. (a) Original simulated ISAR images; (b) the generated ISAR images.

To quantitatively evaluate the quality of generated ISAR images, we use the structural similarity (SSIM) [11]. It measures the similarity of the two images in luminance (I), contrast (C), and structure (S) together[12]:

$$I(x,y) = \frac{2\mu_x\mu_y + C_1}{\mu_x^2 + \mu_y^2 + C_1} \tag{3}$$

$$C(x,y) = \frac{2\sigma_x\sigma_y + C_2}{\sigma_x^2 + \sigma_y^2 + C_2} \tag{4}$$

$$S(x,y) = \frac{\sigma_{xy} + C_3}{\sigma_x\sigma_y + C_3} \tag{5}$$

Where x, y are two images that to be compared, μ_x, μ_y is the mean of pixel intensity and σ_x, σ_y are the standard deviations of pixel intensity.σ_{xy} is the correlation coefficient between corresponding pixels in x and y. And SSIM is defined as:

$$\mathrm{SSIM}(x,y) = I(x,y)^{\alpha} C(x,y)^{\beta} S(x,y)^{\gamma} \tag{6}$$

When two images are exactly same, the SSIM value reaches the maximum of 1. We evaluate the SSIM of the generated and the simulated images of eight aircrafts, respectively, and the mean SSIM of each category are shown

in Table II. In general, the generated images are consistent with the simulated ones (SSIM is larger than 0.7). The SSIM scores range from 0.7127 to 0.8990. Besides, we find that the quality of small aircrafts (Airbus-220 and Airbus-320) is better than the large ones.

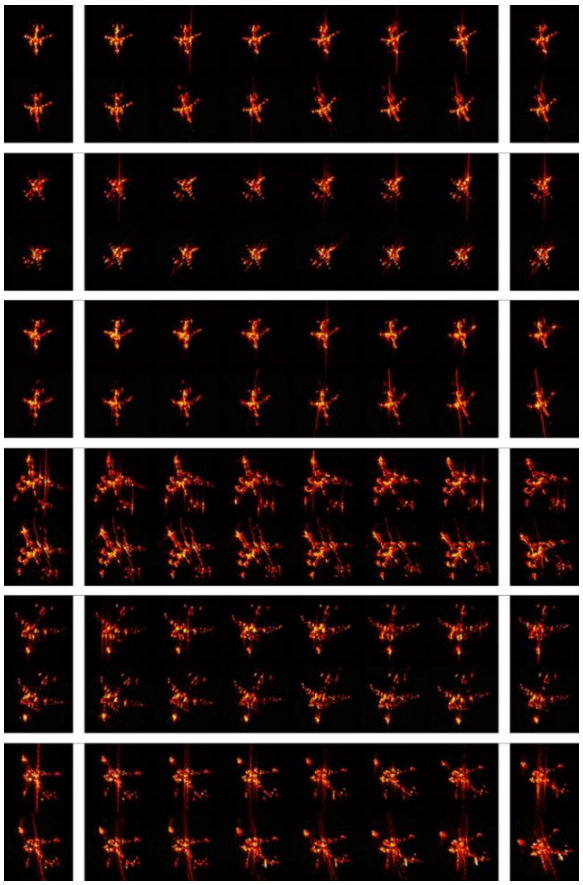

Fig. 7. Network generation result (expand the ISAR dataset by interpolating the orientation angle).

Table II SSIM scores of the generated and simulated images.

Category	SSIM
Airbus-220	0.8603
Airbus-320	0.8990
Boieng-737	0.8672
Boieng-747	0.7127
Boieng-777	0.7903
Boieng-787	0.7735

5. CONCLUSION

In this paper, we proposed an ISAR images generative network, which is validated by a simulated ISAR images dataset. Results demonstrate the high effectivity of the proposed method in expanding the ISAR images dataset along orientation dimension. The SSIM of generated and simulated images is larger than 0.7 for all the eight types of aircrafts. Thus, we believe that the proposed method has great application potential in augmenting the training samples.

6. ACKNOWLEDGMENT

This work was supported in part by the National Natural Science Foundation of China (Grant No. 61901122), the Natural Science Foundation of Shanghai (Grant No. 20ZR1406300) and the Science Foundation of the Shanghai Academy of Spaceflight Technology (SAST 2019-073).

REFERENCES

[1] F. Wang, T. F. Eibert, and Y. Jin, "Simulation of ISAR Imaging for a Space Target and Reconstruction Under Sparse Sampling via Compressed Sensing," *IEEE Transactions on Geoscience and Remote Sensing,* vol. 53, no. 6, pp. 3432-3441, 2015.

[2] S. Chen, H. Wang, F. Xu, and Y. Jin, "Target Classification Using the Deep Convolutional Networks for SAR Images," *IEEE Transactions on Geoscience and Remote Sensing,* vol. 54, no. 8, pp. 4806-4817, 2016.

[3] I. J. Goodfellow *et al.*, "Generative adversarial nets," presented at the Proceedings of the 27th International Conference on Neural Information Processing Systems - Volume 2, Montreal, Canada, 2014.

[4] Q. Song, F. Xu, and Y. Jin, "SAR Image Representation Learning With Adversarial Autoencoder Networks," in *IGARSS 2019*, 2019, pp. 9498-9501.

[5] M. Mirza and S. Osindero, "Conditional generative adversarial nets," *arXiv preprint arXiv:1411.1784,* 2014.

[6] J. Hwang, C. Yu, and Y. Shin, "SAR-to-Optical Image Translation Using SSIM and Perceptual Loss Based Cycle-Consistent GAN," in *2020 International Conference on Information and Communication Technology Convergence (ICTC)*, 2020, pp. 191-194.

[7] H. Huang, F. Zhang, Y. Zhou, Q. Yin, and W. Hu, "High Resolution SAR Image Synthesis with Hierarchical Generative Adversarial Networks," in *IGARSS 2019*, 2019, pp. 2782-2785.

[8] F. Xu and Y. Jin, "Bidirectional Analytic Ray Tracing for Fast Computation of Composite Scattering From Electric-Large Target Over a Randomly Rough Surface," *IEEE Transactions on Antennas and Propagation,* vol. 57, no. 5, pp. 1495-1505, 2009.

[9] T. Karras, T. Aila, S. Laine, and J. Lehtinen, "Progressive growing of gans for improved quality, stability, and variation," in *ICLR 2018*, Vancouver, Canada, 2018, pp. 1-26.

[10] I. Gulrajani, F. Ahmed, M. Arjovsky, V. Dumoulin, and A. Courville, "Improved Training of Wasserstein GANs," *Advances in Neural Information Processing Systems,* pp. 5767-5777, 03/31 2017.

[11] W. Zhou, A. C. Bovik, H. R. Sheikh, and E. P. Simoncelli, "Image quality assessment: from error visibility to structural similarity," *IEEE Transactions on Image Processing,* vol. 13, no. 4, pp. 600-612, 2004.

[12] A. Borji, "Pros and cons of gan evaluation measures," *Computer Vision and Image Understanding,* vol. 179, pp. 41-65, 2019.